^{68}Ga-PSMA-11 PET/MR Detects Local Recurrence Occult on mpMRI in Prostate Cancer Patients After HIFU

Irene A. Burger[1], Julian Müller[1], Olivio F. Donati[2], Daniela A. Ferraro[1], Michael Messerli[1], Benedikt Kranzbühler[3], Edwin E.G.W. ter Voert[1,4], Urs J. Muehlematter[1], Niels J. Rupp[5], Ashkan Mortezavi[3], and Daniel Eberli[3]

[1]Department of Nuclear Medicine, University Hospital Zürich, Zürich, Switzerland; [2]Institute of Diagnostic and Interventional Radiology, University Hospital Zürich, Zürich, Switzerland; [3]Department of Urology, University Hospital Zürich, Zürich, Switzerland; [4]University of Zurich, Zürich, Switzerland; and [5]Department of Pathology and Molecular Pathology, University Hospital Zürich, Zürich, Switzerland

High-intensity focused ultrasound (HIFU) is a promising new modality for the treatment of localized prostate cancer (PCa). Follow-up of patients is recommended with biopsies and multiparametric MRI (mpMRI). However, mpMRI in the postinterventional setting is often false-negative. It was our aim to investigate if the new tracer targeting the prostate-specific membrane antigen (^{68}Ga-PSMA-11) could be used to localize recurrent disease with PET/MR in patients with discrepant findings between mpMRI and template biopsies. **Methods:** Interim analysis was performed of the first 10 patients scanned between September 2016 and May 2018 with positive template biopsy and negative mpMRI after HIFU from an ongoing clinical trial (NCT02265159). All patients underwent ^{68}Ga-PSMA-11 PET/MRI within 3 mo. Four prostatic quadrants were defined, and for every quadrant suspicion for recurrence was rated on a 5-point Likert scale from definitely no recurrence (1) to highly suspected of recurrence (5), with 4 used as a cutoff for suspected disease based on PET/MRI by a masked reader. ^{68}Ga-PSMA-11 uptake of suspected lesions and background areas was measured with the SUV_{max}. The apparent diffusion coefficient values of lesions and background were given for each segment. PET/MRI scans were compared with the template biopsy results, including corresponding Gleason scores (GS), number of positive cores, and tumor length. **Results:** The quadrant-based sensitivity, specificity, and positive and negative predictive values for PET/MRI were 55%, 100%, 100%, and 85%, respectively. Patient-based PET/MRI was negative in 4 cases with GS 3 + 4 and a tumor length between 0.1 and 3 mm. All tumor lesions with GS 4 + 3 or higher were detected on PET/MRI. **Conclusion:** Our preliminary results indicate that ^{68}Ga-PSMA-11-PET/MR has the potential to localize PCa recurrence after HIFU occult on mpMRI.

Key Words: prostate-specific membrane antigen; magnetic resonance imaging; template biopsy; high-intensity focused ultrasound

J Nucl Med 2019; 60:1118–1123
DOI: 10.2967/jnumed.118.221564

Focal treatment of the prostate with high-intensity focused ultrasound (HIFU) is a promising new modality for the treatment of localized prostate cancer (PCa). With limited side effects such as urinary incontinence and erectile dysfunction, disease control after one treatment can be reached in about 81%–92% of the patients (*1*). There is currently no validated method to monitor treatment success. On the basis of consensus meetings, follow-up of patients to rule out persistence or recurrence is recommended with biopsies, prostate-specific antigen (PSA), and multiparametric MRI (mpMRI) (*2,3*). Prostate biopsies remain the most accurate option to monitor patients after focal HIFU (*4*). However, tissue sampling is an invasive procedure associated with significant morbidity (*5*). So far, the noninvasive diagnostic tests PSA and mpMRI could not show sufficient sensitivity and specificity to replace follow-up biopsies.

The interpretation of mpMRI is often difficult because of signal alterations of the treated prostate. Early work on the MRI appearance of the prostate after HIFU showed focal high signal on T1-weighted images, most likely representing interstitial hemorrhages, and a dark central zone on T2-weighted images representing the central necrosis (*6*). The same authors suggested later that dynamic contrast enhancement can increase the detection of local recurrence after HIFU (*2*). But still, the postinterventional changes, especially the focal hemorrhages, can limit the interpretation of mpMRI for prostate (*7*).

The novel PET tracer targeting the prostate-specific membrane antigen (PSMA) labeled with ^{68}Ga (^{68}Ga-PSMA-11) is primarily used for the detection of recurrent PCa (*8,9*). The major benefit of ^{68}Ga-PSMA-11 is a significantly improved sensitivity (*10*), with a high reliability and robust interreader agreement (*11,12*). First investigations showed that ^{68}Ga-PSMA-11 can also be used to improve local staging of PCa (*13,14*), corresponding to the initial results on immunohistochemistry showing a low PSMA expression on the cell membrane in normal prostate tissue but high membranous expression on PCa (*15*).

The effect of focal HIFU on PSMA expression is unknown. Until now, only one case report describing a successful re-HIFU based on a positive choline PET/MRI has been published (*16*). However, the limited specificity of choline in the prostate limits the confidence in choline PET/MR as a tool for reevaluation after HIFU, since not only PCa but also benign prostate hyperplasia is known to have intense choline uptake. ^{68}Ga-PSMA-11 does not

Received Oct. 11, 2018; revision accepted Dec. 19, 2018.
For correspondence or reprints contact: Irene A. Burger, Department of Nuclear Medicine, University Hospital Zürich, Rämistrasse 100, 8091 Zürich, Switzerland.
E-mail: irene.burger@usz.ch
Published online Jan. 25, 2019.
COPYRIGHT © 2019 by the Society of Nuclear Medicine and Molecular Imaging.

have increased uptake in benign prostate hyperplasia and might be superior for the detection of local recurrence after HIFU.

Therefore, we investigated if ^{68}Ga-PSMA-11 PET/MRI could be used to localize biopsy-proven recurrent disease after HIFU therapy in patients with negative mpMRI.

MATERIALS AND METHODS

Patients

We performed an interim analysis of the first 10 patients prospectively investigated between December 2016 and March 2018 from an ongoing prospective single-arm clinical trial (NCT02265159). All patients underwent curatively intended focal HIFU therapy for a Gleason score (GS) 6–7 PCa. Patients were included and referred for a ^{68}Ga-PSMA-11 PET/MRI scan of the pelvis if there was a biopsy-proven significant PCa on transperineal follow-up template biopsy, not detected on clinical routine mpMRI. The maximum interval accepted between biopsy and mpMRI was 3 mo. PCa was defined as clinically significant in the presence of any Gleason 4 pattern (GS $\geq$ 3 + 4).

Template Biopsy of the Prostate

Systematic transperineal template mapping fusion biopsies were performed by experienced urologists in all patients after 6, 12, and 36 mo after initial HIFU therapy. Patients were placed in the dorsal lithotomy position. As an antibiotic prophylaxis, all patients received 80 mg of gentamycin intravenously before biopsy. Fusion of live transrectal ultrasound and mpMRI was performed using the BiopSee biopsy system (Medcom) to allow later reconstruction of the histology. Systematic biopsy cores were taken from all 20 predefined Barzell zones, leading to organ coverage of approximately 95% (*17*). For comparison to the PSMA PET/MRI results, the biopsy cores were grouped into 4 quadrants: right anterior, left anterior, right posterior, and left posterior.

^{68}Ga-PSMA-11 PET/MRI

All patients underwent pelvic PET/MRI on a dedicated hybrid scanner (Signa PET/MR; GE Healthcare) 60 min after injection of 85 MBq ^{68}Ga-PSMA-11 (range, 82–89 MBq). The protocol included specific sequences covering the pelvis, including a high-resolution T1-weighted liver acquisition with volume acquisition (LAVA)-FLEX sequence, a T2-weighted fast recovery fast spin-echo sequence in 3 planes, and diffusion-weighted images as previously published (*18*). The PET frame time over the prostate was 15 min; this allowed us to lower the injected dose to 85 MBq of ^{68}Ga-PSMA-11, with excellent image quality. To rule out lymph nodes or distant metastasis, one more partial body frame with a 4-min frame time was performed up to the renal vessels. To reduce ^{68}Ga-PSMA-11 activity in the bladder, furosemide was injected intravenously 30 min before the ^{68}Ga-PSMA-11 injection. Volumes of interest were placed over the entire PSMA-positive lesion tumor. ^{68}Ga-PSMA-11 uptake was quantified with SUV_{max}; furthermore, PSMA uptake in normal prostate tissue was measured.

mpMRI

MRI was performed on a 3-T system (Skyra; Siemens Healthcare). For signal reception, an 18-channel phased-array receiver coil was used. The protocol and the sequence parameters were in concordance with the current international prostate MR guidelines (*19*). Transverse diffusion-weighted echo-planar images, based on dynamic parallel transmit technology, using selective excitation for depiction of a reduced field of view, were acquired with identical orientation and at identical locations to the T2-weighted images with the following acquisition parameters: repetition time/echo time, 5,000/75 ms; in-plane resolution, 0.7 × 0.7 mm; slice thickness, 3 mm; b-values, 100/600/1,000 s/mm^2. Dynamic contrast-enhanced images were acquired using the following parameters: repetition time/echo time, 5–6.3/1.8 ms; in-plane resolution, 1 × 0.6 mm; temporal resolution, less than 8 s. All scans were technically adequate; no patients were excluded from further analysis.

Image Analysis

Two readers, one with 10 y and one with 2 y of experience in urogenital imaging, masked to the biopsy results read the PET/MR images. The prostate was subdivided into 8 segments: right anterior base, left anterior base, right posterior base, and left posterior base, with corresponding segments at the apex. For every segment, suspicion of recurrence was rated on a 5-point Likert scale from no recurrence (*1*) to highly suspected of recurrence (*5*), with 3 and 4 used as a cutoff for suspected recurrence.

For quantitative analysis, images were directly compared with the biopsy results, and for every PCa lesion with GS greater than 3 + 3, the corresponding SUV_{max} and apparent diffusion coefficient (ADC) values were assessed for the corresponding region.

For every lesion, the modified GS according to the World Health Organization 2016 classification (*20*), the number of positive cores, and the maximum cancer core length in millimeters were recorded. To compare the total tumor burden with the corresponding quantitative ^{68}Ga-PSMA-11 PET/MR and mpMRI metrics, the cancer volume was estimated by multiplication of the number of positive cores and maximum core length in millimeters.

Patients were included in the presence of any Gleason 4 pattern; however, additional definitions of clinical significance based on the definition of Ahmed et al. used in the PROMIS trial were applied to improve the comparability with published literature (GS $\geq$ 4 + 3 or a maximum cancer core length of 6 mm or longer) (*21*).

TABLE 1
Patient Characteristics

Characteristic	Value
Age (y)	
Mean ± SD	68 ± 4.3
Range	60–75
PSA (pre-HIFU)	
Mean ± SD	6.4 ± 3.5
Range	1.5–12.7
GS (pre-HIFU)	
3 + 4	4 (40%)
4 + 3	6 (60%)
PSA (at scan)	
Mean ± SD	3.1 ± 2.2
Range	0.7–7.6
Time between HIFU and recurrence	
Mean ± SD	15.8 ± 9.4
Range	6.2–35.3
GS (at scan on template biopsy)	
3 + 4	6
4 + 3	3
4 + 4	1

Total number of patients is 10.

TABLE 2
Segment-Based Sensitivity and Specificity

Parameter	TP	TN	FP	FN	Sens	Spec	PPV	NPV
PSMA PET/MRI (4/5)	6	29	0	5	55%	100%	100%	85%
PSMA PET/MRI (3–5)	6	28	1	5	55%	97%	86%	85%

TP = true positive; TN = true negative; FP = false positive; FN = false negative; Sens = sensitivity; Spec = specificity; PPV = positive predict value; NPV = negative predict value.

Statistical Analysis

Statistical analyses were performed using SPSS statistics software, version 23 (IBM). The 8 segments form the qualitative image analysis were aggregated into quadrants by summarizing corresponding locations from the base and the apex as previously reported (*22*). Interreader agreement was assessed with weighted κ. Calculation of sensitivity and specificity was quadrant-based, after dichotomization of both imaging and pathology data and summarizing the imaging results for apex and base. Pathology was considered positive for significant cancer harboring a GS of more than 3 + 3, and imaging interpretation was considered positive for a score of 4–5 or 3–5. Descriptive analyses were used to display patient data as mean and range. The correlation between estimated tumor volume and SUV_{max} and ADC values was assessed with a 2-tailed Pearson correlation test. A P value of less than 0.05 was considered statistically significant.

RESULTS

The median age was 68 y (range, 60–75 y). The median interval between focal HIFU and positive transperineal template biopsy was 16 mo (range, 6–35 mo), and the median interval between mpMRI and ^{68}Ga-PSMA-11 PET/MRI was 2 mo (range, 0–3 mo). All routine interpretations of mpMRI were negative for recurrent disease. In 6 patients, GS 3 + 4 lesions were detected, 3 patients had GS 4 + 3 disease, and 1 patient had GS 4 + 4. Patient characteristics are given in Table 1.

Patient-Based Analysis

For 6 of 10 patients, the ^{68}Ga-PSMA-11 PET/MRI was positive, with complete agreement for both readers. No false-positive lesions were seen on ^{68}Ga-PSMA-11 PET/MRI. Five of the lesions were given a Likert score of 5 (highly suspected recurrence), and in one case a score of 4 (probably recurrence) was given. No patient had suspected lesions outside the prostate.

Quadrant-Based Lesion Detection on ^{68}Ga-PSMA-11 PET

The quadrant-based sensitivity, specificity, and positive and negative predictive values for ^{68}Ga-PSMA-11 PET/MRI were 55%, 100%, 100%, and 85%, respectively. The weighted interreader agreement for the 5-point scale was a κ value of 0.78 (confidence interval, 0.68–0.94). Six suspected lesions were seen on ^{68}Ga-PSMA-11 PET/MRI by both readers, all corresponding to the quadrant positive for PCa on template biopsy. Four lesions were not detected on ^{68}Ga-PSMA-11 PET/MRI in the masking reading. All lesions negative on PET had GS 3 + 4 disease with only 1 core positive and a maximum core length of less than 4 mm. After dichotomization, there was full agreement between both readers. By reader 1, only one segment labeled as undetermined on ^{68}Ga-PSMA-11 PET/MRI (Likert score 3) was negative on pathology (Table 2).

Illustrations are provided of 2 lesions, one positive (Fig. 1) and one negative (Fig. 2) on ^{68}Ga-PSMA-11 PET/MRI.

Correlation of ^{68}Ga-PSMA-11 PET Uptake and Diffusion Restriction with Tumor Burden

According to the definition of significant cancer used in the PROMIS trial by Ahmed et al. (defined as a Gleason of 4 + 3 or more, or a maximum cancer core length of 6 mm or more) (*21*), only 3 patients had clinically significant tumor; all were positive on ^{68}Ga-PSMA-11 PET with a mean SUV_{max} 8.4.

If any Gleason pattern 4 is considered clinically significant, the median uptake on ^{68}Ga-PSMA-11 PET–positive cancer lesions is SUV_{max} 8.6 (range from 4.6 to 12.1, Table 3).

Higher estimated tumor volume (defined as the number of positive biopsies multiplied by maximum core length) and higher GS were associated with ^{68}Ga-PSMA-11 uptake, measured as SUV_{max} or tumor-to-background ratio (Fig. 3). There was a significant correlation between estimated tumor volume and SUV_{max} (0.674, $P < 0.001$).

The median maximum ^{68}Ga-PSMA-11 uptake in the negative segments had an SUV_{max} of 3.5 (range from 2.2 to 5.8). High ^{68}Ga-PSMA-11 accumulation ($SUV_{max} >$ 4) was observed in 7 segments in the posterior base, corresponding to increased activity in the central zone, and not rated as suspected of recurrence.

Comparing the ADC values with the estimated tumor volume and GS, there was no association between lower ADC values and higher GS or estimated tumor volume (Fig. 4). There was no significant correlation between estimated tumor volume and ADC values (0.040, $P = 0.808$). ADC values were slightly lower in segments positive

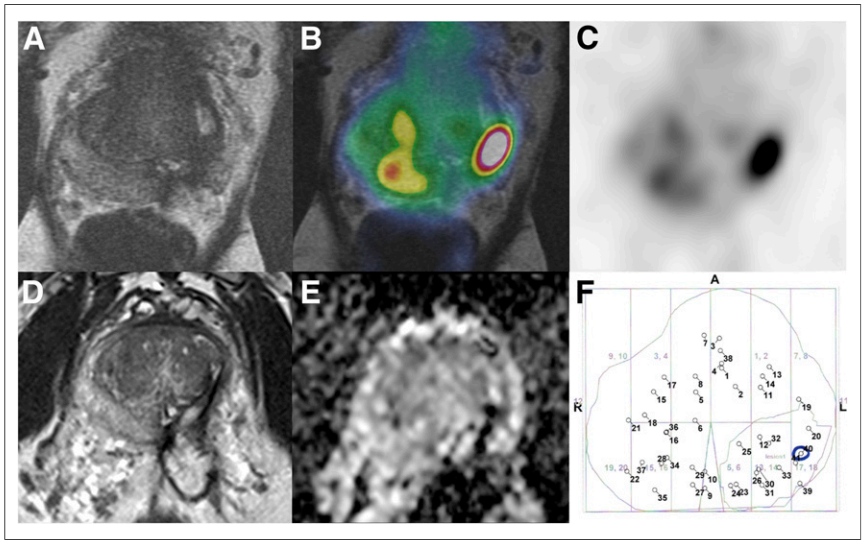

FIGURE 1. First patient (HK06). (A–C) Axial slices of T2-weighted MRI, fused PSMA PET/MRI, and PSMA PET (windows 1–8), with intense uptake in left posterolateral peripheral zone. (D and E) Negative axial mpMRI (T2-weighted MRI and ADC map). (F) Corresponding PDF from BiopSee system with positive core biopsy (GS 4 + 3) labeled in blue in PET-positive area.

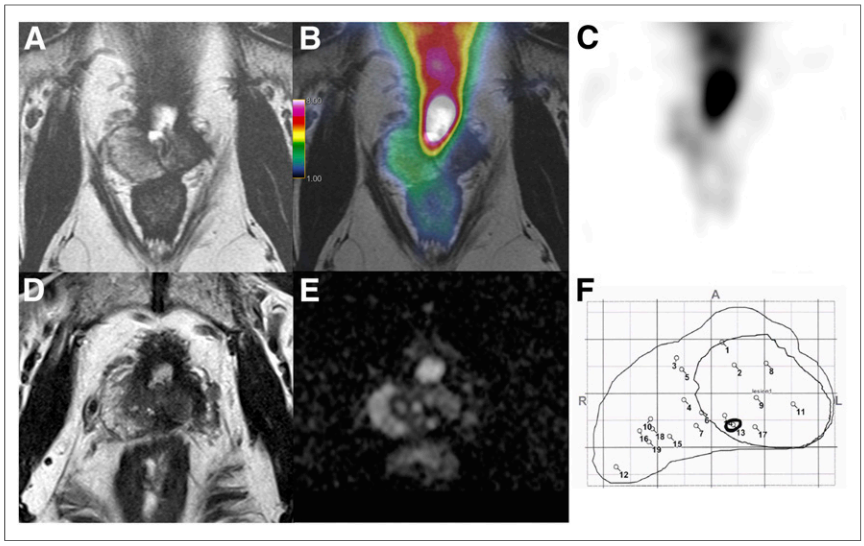

FIGURE 2. Second patient (HK09). (A–C) Axial slices of T2-weighted MRI, fused PSMA PET/MRI, and PSMA PET (windows 1–8), without increased uptake. (D and E) Negative axial mpMRI (T2-weighted MRI and ADC map). (F) PDF from BiopSee system with 1 positive core biopsy (GS 3 + 4) labeled in black.

for PCa (mean, 1,059 ± 560 × 10^{-6} mm^2/s; range, 131–1,811 × 10^{-6} mm^2/s) than in cancer-negative segments, with a mean ADC of 1,174 ± 390 × 10^{-6} mm^2/s (range, 445–2,078 × 10^{-6} mm^2/s).

DISCUSSION

Our study shows that in 6 of 10 patients, ^{68}Ga-PSMA-11 PET/MRI detected recurrent disease not seen on clinical routine mpMRI. Furthermore, PSMA accumulation in true-positive lesions had a high tumor-to-background ratio and correlated significantly with the total tumor burden, whereas ADC values did not show a significant negative correlation with tumor burden.

These results stand in contrast to the previously published excellent results for mpMRI to detect recurrent disease after HIFU therapy, with sensitivities ranging from 94% to 97% (*2,23*). However, all previously published studies used transrectal biopsies with or without MRI guiding as a reference standard. In the study published by Lotte et al., 24 of 98 patients were excluded because they did not undergo any biopsy, as was probably due to a negative mpMRI result (*23*). The use of mpMRI to guide biopsy gained wide acceptance and is ideally performed in patients without previous intervention. After a previous biopsy, the PICTURE study in 249 patients showed that using a Likert score of 3 as a cutoff, the sensitivity for mpMRI is very high (97%), to the price of a very low specificity of 22% (*24*), reflecting the potential false-positive findings in the prostate after interventions (*7*).

Furthermore, these results for the accuracy of mpMRI to detect clinically significant cancer were based on the definition according to Ahmed et al.: a GS of at least 4 + 3 or a maximum cancer core length of at least 6 mm (*21,25*). Applying the same threshold to our study, we found that only 3 patients had significant tumor on template biopsy; ^{68}Ga-PSMA-11 PET/MR was positive in all 3 cases, whereas mpMRI was not able to detect those lesions.

In the setting of focal therapy, not only detection but also accurate delineation of the tumor are crucial for potential retreatment. In a recent analysis of 625 consecutive patients undergoing HIFU therapy, a high failure-free 5-y survival of 88% was achieved. Even patients with a high-risk tumor according to the D'Amico classification did not need salvage therapy or show any metastasis 5 y after HIFU (*26*). In this multicenter study, only 222 of 625 patients underwent biopsies after HIFU, and a PSA rise was not considered an endpoint for failure-free survival. The authors do not state whether mpMRI was performed routinely, but in 121 of the patients a repeat HIFU was performed (*26*). The optimal surveillance after focal prostate therapy is still controversial. A

TABLE 3
Overview for Pathology (Template Biopsy), PSMA, and ADC Values

Patient	GS	Pos cores	MCL (mm)	Clin sig Ca	SUV_{max} lesion TP	SUV_{max} BG	Lesion/BG	ADC (×10^{-6} mm^2/s)
HK01	3 + 4	1	3	N	NA	3.1	NA	1,400
HK02	3 + 4	2	2	N	7.4	3.1	2.4	131
HK03	4 + 4	2	3	Y	8.5	3.8	2.2	1,481
HK04	3 + 4	2	2	N	8.6	3.5	2.5	1,811
HK05	4 + 3	2	2	Y	4.6	2.2	2.1	1,337
HK06	4 + 3	1	4	Y	12.1	3.6	3.4	1,430
HK07	3 + 4	1	2	N	NA	3.5	NA	493
HK08	3 + 4	1	1	N	NA	3.5	NA	1,528
HK09	3 + 4	1	0.1	N	NA	3.2	NA	414
HK10	3 + 4	1	1	N	9.9	3.2	3.1	564

Pos cores = number of positive biopsy cores; MCL = maximum core length; Clin sig Ca = clinically significant cancer according to Ahmed et al. (*21*); TP = true positive; BG = background; NA = not applicable.

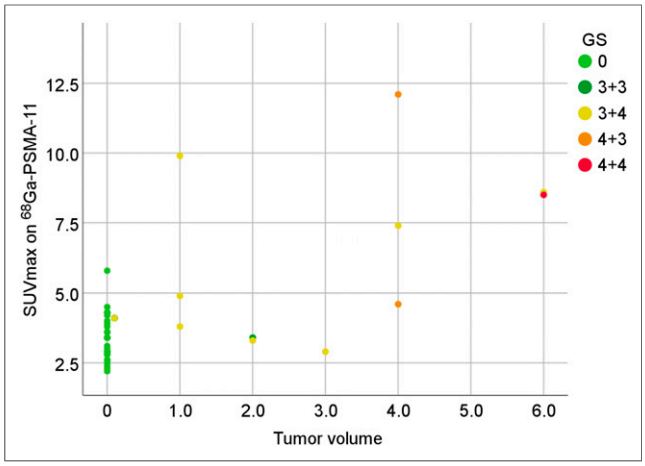

FIGURE 3. Scatterplot for estimated tumor volume (number of positive biopsies multiplied by maximum core length) and uptake on ^{68}Ga-PSMA-11 PET (SUV_{max}) showing significant correlation between estimated tumor volume and SUV_{max} ($r = 0.674$, $P < 0.001$), as well as association with higher GS represented by colors and increased uptake on ^{68}Ga-PSMA-11 PET.

recently published metaanalysis and consensus publication suggests that mpMRI should be performed at 3–6 mo (with targeted biopsy of the treated zone and any suspected lesion seen on mpMRI), at 12–24 mo, and at 5 y. Additionally, a systematic biopsy should be performed at 12–24 mo and again at 5 y (*4*). The sensitivity of mpMRI for the detection of clinically relevant cancer in comparison to template biopsies was based on studies in men without any focal treatment (*27–29*). Indeed, little is known about the sensitivity of mpMRI, especially early after HIFU, when postinterventional changes are still present. The consensus recommendations published in 2013 state that mpMRI is the technique of choice for follow-up of focal ablation. Early publications of mpMRI after HIFU revealed extensive signal alterations after 3 and 6 mo, with low signal on T2-weighted images and a substantial decrease in volume, but observed that contrast enhancement might correlate with residual disease (*30*). However, the most recent paper, on 45 patients undergoing mpMRI and transrectal ultrasound–guided biopsy after HIFU, concluded that dynamic contrast enhancement did not add any information compared with T2-weighted imaging and diffusion (*23*). However, this result needs to be considered with caution, since many patients (24/98) with negative mpMRI results were not considered for transrectal ultrasound–guided biopsy within the study protocol.

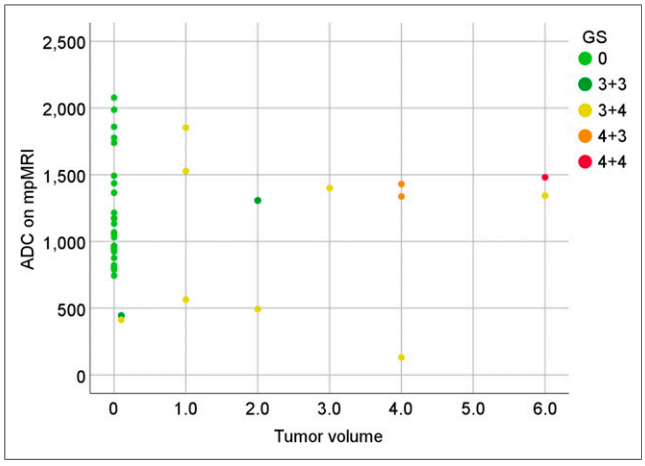

FIGURE 4. Scatterplot for estimated tumor volume (number of positive cores multiplied by maximum core length) and ADC values ($\times 10^{-6}$ mm^2/s) from mpMRI did not show significant correlation with estimated tumor volume ($r = 0.040$, $P = 0.808$) or association between higher GS and lower ADC values.

The first results with a high detection of clinically significant cancer with PSMA PET/MR (*13,14*) have now been further supported by recent studies showing a good correlation between PSMA uptake and GS or PSA values (*31,32*). However, not every PCa has a high PSMA expression; in fact, early immunohistochemistry work has shown that around 10% of PCa cases do not express PSMA (*15,33*). This finding is in concordance with present results from large studies with more than 100 patients for recurrent PCa, where PSMA PET reaches detection rates of 89%–97% for a PSA value above 2 ng/mL (*34*). Therefore, in a small portion of about 10% of the patients, PSMA PET might be of limited use. For patients without PSMA expression, alternative tracers such as ^{68}Ga-bombesin, targeting the gastrin-releasing peptide receptor (*35,36*), could be investigated for optimized personalized tumor detection and early therapy.

Our study has limitations, as it is a selected subgroup of patients with a positive biopsy but a negative clinical mpMRI result after HIFU. With the present data, it cannot be excluded that in some cases the clinical mpMRI would be positive and PSMA PET false-negative; an overall sensitivity and specificity for both modalities after HIFU can therefore not be calculated. Given that patients within the HIFU study protocol already undergo multiple interventions and scans, it was the aim of this preliminary study to investigate if patients with discrepant findings between mpMRI and template biopsies could profit from the additional ^{68}Ga-PSMA-11 PET/MRI to localize significant tumor. The promising results now will lead to a larger study investigating all patients with mpMRI and ^{68}Ga-PSMA-11 PET/MRI before template biopsy to shed more light on the potential benefit of ^{68}Ga-PSMA-11 PET/MRI to localize persistent or recurrent cancer in the prostate after focal therapy.

CONCLUSION

Our preliminary results indicate that ^{68}Ga-PSMA-11 PET/MR might detect local recurrence of PCa after HIFU that is not detected by mpMRI. ^{68}Ga-PSMA-11 PET/MRI could be used to plan and target secondary HIFU to increase the rate of disease control for this promising new focal therapy.

DISCLOSURE

Irene Burger has received research grants from GE Healthcare, the Iten-Kohaut Foundation, and Swiss Life and a speaker honorarium from GE Healthcare, Bayer Health Care, and Astellas Pharma AG. The Department of Nuclear Medicine holds an institutional research contract with GE Healthcare. The Sick Legat and the Iten-Kohaut Foundations provided financial support. No other potential conflict of interest relevant to this article was reported.

ACKNOWLEDGMENTS

We acknowledge the technicians Marlena Hofbauer, Miguel Porto, Sofia Kaltsuni, Melanie Thüringer, Michele Hug, and Sabrina Epp for their excellent work on high-quality PET/MR scans.

REFERENCES

1. Blana A, Walter B, Rogenhofer S, Wieland WF. High-intensity focused ultrasound for the treatment of localized prostate cancer: 5-year experience. *Urology.* 2004;63:297–300.
2. Rouvière O, Girouin N, Glas L, et al. Prostate cancer transrectal HIFU ablation: detection of local recurrences using T2-weighted and dynamic contrast-enhanced MRI. *Eur Radiol.* 2010;20:48–55.
3. Muller BG, van den Bos W, Brausi M, et al. Follow-up modalities in focal therapy for prostate cancer: results from a Delphi consensus project. *World J Urol.* 2015;33:1503–1509.
4. Tay KJ, Amin MB, Ghai S, et al. Surveillance after prostate focal therapy. *World J Urol.* 2019;37:397–407.
5. Loeb S, Vellekoop A, Ahmed HU, et al. Systematic review of complications of prostate biopsy. *Eur Urol.* 2013;64:876–892.
6. Rouvière O, Lyonnet D, Raudrant A, et al. MRI appearance of prostate following transrectal HIFU ablation of localized cancer. *Eur Urol.* 2001;40:265–274.
7. Rosenkrantz AB, Taneja SS. Radiologist, be aware: ten pitfalls that confound the interpretation of multiparametric prostate MRI. *AJR.* 2014;202:109–120.
8. Afshar-Oromieh A, Holland-Letz T, Giesel FL, et al. Diagnostic performance of ^{68}Ga-PSMA-11 (HBED-CC) PET/CT in patients with recurrent prostate cancer: evaluation in 1007 patients. *Eur J Nucl Med Mol Imaging.* 2017;44:1258–1268.
9. Maurer T, Murphy DG, Hofman MS, Eiber M. PSMA-PET for lymph node detection in recurrent prostate cancer: how do we use the magic bullet? *Theranostics.* 2017;7:2046–2047.
10. Maurer T, Gschwend JE, Rauscher I, et al. Diagnostic efficacy of ^{68}gallium-PSMA positron emission tomography compared to conventional imaging for lymph node staging of 130 consecutive patients with intermediate to high risk prostate cancer. *J Urol.* 2016;195:1436–1443.
11. Fanti S, Minozzi S, Morigi JJ, et al. Development of standardized image interpretation for ^{68}Ga-PSMA PET/CT to detect prostate cancer recurrent lesions. *Eur J Nucl Med Mol Imaging.* 2017;44:1622–1635.
12. Fendler WP, Calais J, Allen-Auerbach M, et al. ^{68}Ga-PSMA-11 PET/CT interobserver agreement for prostate cancer assessments: an international multicenter prospective study. *J Nucl Med.* 2017;58:1617–1623.
13. Park SY, Zacharias C, Harrison C, et al. Gallium 68 PSMA-11 PET/MR imaging in patients with intermediate- or high-risk prostate cancer. *Radiology.* 2018;288: 495–505.
14. Eiber M, Weirich G, Holzapfel K, et al. Simultaneous ^{68}Ga-PSMA HBED-CC PET/MRI improves the localization of primary prostate cancer. *Eur Urol.* 2016;70:829–836.
15. Silver DA, Pellicer I, Fair WR, Heston WD, Cordon-Cardo C. Prostate-specific membrane antigen expression in normal and malignant human tissues. *Clin Cancer Res.* 1997;3:81–85.
16. Burger IA, Gafita A, Muller J, Kranzbuhler B, Donati OF, Eberli D. ^{18}F-choline PET/MR can detect and delineate local recurrence after high-intensity focused ultrasound therapy of prostate cancer. *Clin Nucl Med.* 2018;43:e111–e112.
17. Mortezavi A, Marzendorfer O, Donati OF, et al. Diagnostic accuracy of multiparametric magnetic resonance imaging and fusion guided targeted biopsy evaluated by transperineal template saturation prostate biopsy for the detection and characterization of prostate cancer. *J Urol.* 2018;200:309–318.
18. Kranzbühler B, Nagel H, Becker AS, et al. Clinical performance of ^{68}Ga-PSMA-11 PET/MRI for the detection of recurrent prostate cancer following radical prostatectomy. *Eur J Nucl Med Mol Imaging.* 2018;45:20–30.
19. Weinreb JC, Barentsz JO, Choyke PL, et al. PI-RADS prostate imaging—reporting and data system: 2015, version 2. *Eur Urol.* 2016;69:16–40.
20. Humphrey PA, Moch H, Cubilla AL, Ulbright TM, Reuter VE. The 2016 WHO classification of tumours of the urinary system and male genital organs-part B: prostate and bladder tumours. *Eur Urol.* 2016;70:106–119.
21. Ahmed HU, El-Shater Bosaily A, Brown LC, et al. Diagnostic accuracy of multiparametric MRI and TRUS biopsy in prostate cancer (PROMIS): a paired validating confirmatory study. *Lancet.* 2017;389:815–822.
22. Barth BK, De Visschere PJL, Cornelius A, et al. Detection of clinically significant prostate cancer: short dual-pulse sequence versus standard multiparametric MR imaging—a multireader study. *Radiology.* 2017;284:725–736.
23. Lotte R, Lafourcade A, Mozer P, et al. Multiparametric MRI for suspected recurrent prostate cancer after HIFU: is DCE still needed? *Eur Radiol.* 2018;28: 3760–3769.
24. Simmons LAM, Kanthabalan A, Arya M, et al. The PICTURE study: diagnostic accuracy of multiparametric MRI in men requiring a repeat prostate biopsy. *Br J Cancer.* 2017;116:1159–1165.
25. Ahmed HU, Hu Y, Carter T, et al. Characterizing clinically significant prostate cancer using template prostate mapping biopsy. *J Urol.* 2011;186:458–464.
26. Guillaumier S, Peters M, Arya M, et al. A multicentre study of 5-year outcomes following focal therapy in treating clinically significant nonmetastatic prostate cancer. *Eur Urol.* 2018;74:422–429.
27. Arumainayagam N, Ahmed HU, Moore CM, et al. Multiparametric MR imaging for detection of clinically significant prostate cancer: a validation cohort study with transperineal template prostate mapping as the reference standard. *Radiology.* 2013;268:761–769.
28. Rosenkrantz AB, Mendrinos S, Babb JS, Taneja SS. Prostate cancer foci detected on multiparametric magnetic resonance imaging are histologically distinct from those not detected. *J Urol.* 2012;187:2032–2038.
29. Thompson JE, Moses D, Shnier R, et al. Multiparametric magnetic resonance imaging guided diagnostic biopsy detects significant prostate cancer and could reduce unnecessary biopsies and over detection: a prospective study. *J Urol.* 2014;192:67–74.
30. Kirkham AP, Emberton M, Hoh IM, Illing RO, Freeman AA, Allen C. MR imaging of prostate after treatment with high-intensity focused ultrasound. *Radiology.* 2008;246:833–844.
31. Koerber SA, Utzinger MT, Kratochwil C, et al. ^{68}Ga-PSMA-11 PET/CT in newly diagnosed carcinoma of the prostate: correlation of intraprostatic PSMA uptake with several clinical parameters. *J Nucl Med.* 2017;58:1943–1948.
32. Uprimny C, Kroiss AS, Decristoforo C, et al. ^{68}Ga-PSMA-11 PET/CT in primary staging of prostate cancer: PSA and Gleason score predict the intensity of tracer accumulation in the primary tumour. *Eur J Nucl Med Mol Imaging.* 2017;44: 941–949.
33. Marchal C, Redondo M, Padilla M, et al. Expression of prostate specific membrane antigen (PSMA) in prostatic adenocarcinoma and prostatic intraepithelial neoplasia. *Histol Histopathol.* 2004;19:715–718.
34. Perera M, Papa N, Christidis D, et al. Sensitivity, specificity, and predictors of positive ^{68}Ga-prostate-specific membrane antigen positron emission tomography in advanced prostate cancer: a systematic review and meta-analysis. *Eur Urol.* 2016;70:926–937.
35. Kähkönen E, Jambor I, Kemppainen J, et al. In vivo imaging of prostate cancer using [^{68}Ga]-labeled bombesin analog BAY86-7548. *Clin Cancer Res.* 2013;19:5434–5443.
36. Schroeder RP, van Weerden WM, Krenning EP, et al. Gastrin-releasing peptide receptor-based targeting using bombesin analogues is superior to metabolism-based targeting using choline for in vivo imaging of human prostate cancer xenografts. *Eur J Nucl Med Mol Imaging.* 2011;38:1257–1266.